TUD-XPROP isolated propeller performance

Summary

Description	Isolated propeller performance measurements of TUD-XPROP propeller including test setup geometry
License	- Geometry: *CC BY-NC-ND 4.0* - Test data: *CC BY-NC-SA 4.0*
Dependent variables	- Propeller thrust coefficient - Propeller torque coefficient - Propeller efficiency
Independent variables	- Propeller pitch setting - Propeller advance ratio - Freestream velocity (advance ratio sweeps at constant freestream velocity for range of freestream velocities) - Angle of attack (for selected pitch, selected advance ratios)
File contents raw data	Propeller thrust coefficient, power coefficient, efficiency versus advance ratio at symmetric inflow conditions, or versus angle of attack at fixed advance ratio , including wind-tunnel conditions for each data point
File contents RSM coefficients	Response surface models for propeller thrust coefficient, power coefficient as function of advance ratio for each freestream velocity
Date measurements	28-29 August 2017, 24-25 October 2017, 25-26 April 2018
Data files created	5 July 2021
Facility	TUD Open-Jet Facility
Model	TUD-XPROP propeller setup
Tunnel operator(s)	Tom Stokkermans, Nando van Arnhem, Tomas Sinnige
Contact	T.Sinnige@tudelft.nl

Contents

1 License

2 Test Objectives

The isolated propeller performance characteristics of the Delft University of Technology research propeller TUD-XPROP were measured during three separate campaigns with similar objectives, performed in August 2017, October 2017, and April 2018. The goal of these measurements was to:

- Obtain the baseline propeller performance for studies of propeller performance at extreme angles of attack (shared in a separate data set through ae.tudelft.nl/propellerdata);
- Obtain the baseline propeller performance for airframe-integration studies considering the use of swirl-recovery vanes;
- Obtain the baseline propeller performance for airframe-integration studies considering wake-ingesting propellers.

3 Test Configuration

Wind-Tunnel Facility

The experiments were performed in the Open-Jet Facility (OJF) at Delft University of Technology. This low-speed, closed-return open-jet wind tunnel features an octagonal outlet of 2.85 m width and height. The maximum outlet velocity is 30 m/s, with a turbulence level of about 0.5%. The setup was installed on a ground plane, which minimized the local expansion of the jet and thus led to the most uniform inflow conditions possible.

Wind-Tunnel Model

The tests were performed with the 6-bladed TUD-XPROP propeller model with diameter of 0.4064 m (Figure 1). The propeller features six carbon-fiber blades, and has a variable pitch setting. Measurements were performed with pitch setting of 20, 30, and 45 degrees at 70% of the radius. Separate CAD files are provided for the three blade pitch settings. The unswept blades have variable twist, chord, and airfoils in the radial direction (Figure 2). The propeller was driven by a Tech Development Inc. 1999 air motor, with the exhaust flow expelled into the test section. The whole setup was supported by a streamlined strut mounted to the wind-tunnel floor. The setup featured an integrated six-component rotating shaft balance (RSB). This custom-made RSB was connected to the propeller hub to allow for force measurements during operation. A metric fairing was installed on the aft part of the hub to have a streamlined interface between rotating and stationary model components.

Figure 1: TUD-XPROP propeller.

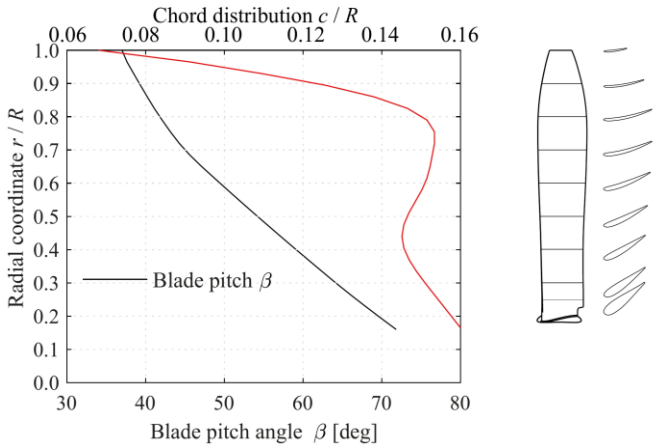

Figure 2: TUD-XPROP planform geometry characteristics.

Test conditions

Measurements were taken for sweeps of the propeller advance ratio at constant freestream velocity. The full range of thrust conditions was considered, ranging from zero thrust to maximum thrust coefficient. To identify scaling effects, for the measurements at 30 deg pitch settings, different freestream velocities were considered, corresponding to Reynolds numbers based on the propeller diameter of 280,000 up to 840,000. With respect to the blade chord at r/R=0.7, the Reynolds number is a function of freestream velocity and advance ratio, and the data set covers values in the range of 85,000 up to 265,000.

Repeated measurements were taken in separate runs to allow for assessment of the repeatability of the measurements. The largest part of the test program was performed with symmetric inflow conditions, with the angle of attack and sideslip both set to 0 degrees. For the pitch setting of 45 degrees, measurements were also taken at nonzero angles of attack ranging from -2 up to 24 degrees.

4 Measurement Equipment

The propeller performance was measured with a rotating shaft balance (RSB), integrated into the propeller hub. This RSB measured the forces on the rotating part of the setup. For this data set only the out-of-plane components, thrust and torque, were recorded. A detailed description of the RSB is provided in [1]. The RSB data were acquired at a sampling rate of 10 kHz, with a measurement time of:

- 15 s for data set at pitch setting of 20 degrees at all conditions (test campaign October 2017)

- 15 s for data set at pitch setting of 30 degrees with freestream velocities of 0, 6, 12, 18 m/s (test campaign October 2017)
- 30 s for data set at pitch setting of 30 degrees with freestream velocities 10, 15, 20, 25, 30 m/s (test campaign August 2017)
- 10 s for data set at pitch setting of 45 degrees at all conditions (test campaign April 2018)

5 Operating Conditions

The propeller performance was expressed in terms of thrust coefficient C_T and power coefficient C_P as a function of advance ratio J, freestream velocity V_∞, tip Mach number M_{tip}, and blade pitch setting at r/R=0.7 $\beta_{0.7R}$. Three different pitch settings were considered. For one of the pitch settings, the angle of attack was also varied. The operating conditions and procedures are summarized below for each pitch setting separately. The exact operating conditions for each test point are included in the data files.

- Data set at $\beta_{0.7R}$=20 deg
  - Sweeps of advance ratio J at zero propeller angle of attack α
    - Advance ratio varied by changing rotational speed varied at four different freestream velocities (same rotational-speed setpoints between freestream velocities)
      - V_∞= 0 m/s: 3400-7000 RPM (7 settings), repeated 4 times (2 up, 2 down)
      - V_∞= 6 m/s: 3400-7000 RPM (7 settings), repeated 3 times (2 up, 1 down)
      - V_∞=12 m/s: 3400-7000 RPM (7 settings), repeated 3 times (2 up, 1 down)
      - V_∞=18 m/s: 3400-7000 RPM (7 settings), repeated 3 times (2 up, 1 down)

- Data set at $\beta_{0.7R}$=30 deg
  - Sweeps of advance ratio J at zero propeller angle of attack α
    - Advance ratio varied by changing rotational speed at five different freestream velocities (same advance-ratio setpoints between freestream velocities)
      - V_∞=10 m/s: 0.40 < J < 1.4 (13 settings), repeated 6 times (3 up, 3 down)
      - V_∞=15 m/s: 0.40 < J < 1.4 (13 settings), repeated 6 times (3 up, 3 down)
      - V_∞=20 m/s: 0.40 < J < 1.4 (13 settings), repeated 6 times (3 up, 3 down)
      - V_∞=25 m/s: 0.45 < J < 1.4 (12 settings), repeated 6 times (3 up, 3 down)
      - V_∞=30 m/s: 0.70 < J < 2.4 (14 settings), repeated 4 times (2 up, 2 down)

- Data set at $\beta_{0.7R}$=45 deg
  - Sweeps of advance ratio J at zero propeller angle of attack α
    - Advance ratio varied by changing rotational speed at single freestream velocity
      - V_∞=29 m/s: 0.55 < J < 1.4 (11 settings), repeated 6 times (3 up, 3 down)
  - Sweeps of propeller angle of attack (α) at constant advance ratio (J)
    - Angle of attack varied at six different advance ratios and single freestream velocity
      - J = 1.4, V_∞=29 m/s: −2 < α < +24 deg (14 settings), repeated 4 times (2 up, 2 down)
      - J = 1.6, V_∞=29 m/s: −2 < α < +25 deg (27 settings), repeated 4 times (2 up, 2 down) (2nd up and downsweeps for −2 < α < +24 deg with 14 settings
      - J = 1.8, V_∞=29 m/s: −2 < α < +24 deg (14 settings), repeated 4 times (2 up, 2 down)
      - J = 2.0, V_∞=29 m/s: −2 < α < +24 deg (14 settings), repeated 4 times (2 up, 2 down)
      - J = 2.2, V_∞=29 m/s: −2 < α < +24 deg (14 settings), repeated 4 times (2 up, 2 down)
      - J = 2.4, V_∞=29 m/s: −2 < α < +24 deg (14 settings), repeated 4 times (2 up, 2 down)

6 Data Processing

6.1 Raw Data Processing

The raw outputs from the RSB were converted into forces and moments using a linear calibration matrix provided by the manufacturer of the RSB. The time histories of forces and moments were time-averaged to obtain the performance estimate for each data point.

6.2 Response-Surface Models

Response-surface models were defined in terms of the following dependent output variables as a function of the following independent variables:

- Thrust coefficient C_T as function of advance ratio J, and propeller angle of attack α only for data set at $\beta_{0.7R}$=45 deg
- Power coefficient C_P as a function of advance ratio J, and propeller angle of attack α only for data set at $\beta_{0.7R}$=45 deg

Linear regression was performed with polynomial models to find the response-surface model that best represented the measured data points in a statistically significant way. The regression procedure was as follows:

- Assume a first-order model and find the best fit.
- Assess the statistical significance of the coefficients. If all statistically significant: increase the order by 1 and redo the regression.
- Continue until at least one of the regression coefficients is no longer statistically significant for two orders in a row. The maximum polynomial order was set to 6 to prevent overfitting.

Confidence intervals were computed from the regression statistics. The confidence interval on the fitted propeller efficiency, a derived quantity, was obtained through propagation of the uncertainties on the models for the thrust and power coefficients.

6.3 Tare Corrections

The zero-loading offset of the RSB was removed from the data by taking tare measurements before and after each polar (usually involving 1 upsweep and 1 downsweep of the independent variable of that polar). Linear interpolation was performed in time to determine the zero-loading offset at each of the test conditions.

The thrust and torque measured with the RSB includes the contributions from the spinner and hub. No attempt was made to remove these force components from the measured data, since the spinner and hub loads with blades off are not representative for the spinner and hub loads with blades present (due to the propeller-induced velocity and pressure gradients).

No correction was performed to account for the back-pressure on the hub.

No correction was performed to account for the impact of the jet from the air motor on the propeller performance.

6.4 Wind-Tunnel Boundary Corrections

The model setup is characterized by small ratios of propeller area to tunnel-outlet area (0.0162) and frontal model area to tunnel-outlet area (0.006), and moderate values of the angle of attack (0-20 deg). Therefore, the corrections due to the effects of the wind-tunnel boundaries are expected to be small and thus are not taken into account.

7 Variable definitions

7.1 Nomenclature

Parameter	***Symbol***	***Unit***
angle of attack	α	deg
angle of sideslip	β	deg
freestream velocity	V_∞	m/s
freestream static temperature	T_∞	K
freestream static pressure	p_∞	Pa
freestream air density	$\rho_\infty = p_\infty/(R \cdot T_\infty)$	kg/m^3
freestream speed of sound	$a_\infty = \sqrt{\gamma \cdot R \cdot T_\infty}$	m/s
propeller rotational speed	n	1/s
tip Mach number	$M_{\text{tip}} = \sqrt{V_\infty^2 + (\pi n D)^2}/a_\infty$	-
propeller advance ratio	$J = V_\infty/nD$	-
propeller diameter	D	m
propeller efficiency	$\eta = \frac{TV_\infty}{P} = J\frac{C_T}{C_P} = \frac{T_C}{P_C}$	-
propeller power	$P = 2\pi \cdot n \cdot Q$	W
propeller power coefficient	$C_P = P/\rho_\infty n^3 D^5$	-
propeller power coefficient	$P_C = P/\rho_\infty V_\infty^3 D^2$	-
propeller thrust	T	N
propeller thrust coefficient	$C_T = T/\rho_\infty n^2 D^4$	-
propeller thrust coefficient	$T_C = T/\rho_\infty V_\infty^2 D^2$	-
propeller torque	Q	Nm

(R = specific gas constant = 287.058, γ = specific heat ratio = 1.4)

7.2 Raw data files

The _rawData files contain the raw data as measured during the experiment. This includes wind-tunnel conditions, propeller operational data, and the relevant propeller performance coefficients. Table 1 provides a description of the contents of the raw data files.

Table 1: Description of the contents of the raw data files.

Parameter	***Description***	***Unit***
polar	polar number	-
DPN	data-point number (of the polar)	-
AoA	angle of attack	deg
AoS	angle of sideslip	deg
V_inf	freestream velocity	m/s
T_inf	freestream static temperature	K

p_inf	freestream static pressure	Pa
rho_inf	freestream air density	kg/m^3
a_inf	freestream speed of sound	m/s
n	propeller rotational speed	1/s
Mtip	tip Mach number	-
J	propeller advance ratio	-
CT	propeller thrust coefficient	-
TC	propeller thrust coefficient	-
CP	propeller power coefficient	-
PC	propeller power coefficient	-
ETA	propeller efficiency	-

7.3 Fitted data files

The _fittedData files contain response-surface models for the following dependent output variables as a function of the following independent variables:

- Thrust coefficient C_T as a function of advance ratio J
- Power coefficient C_P as a function of advance ratio J

The fitted data files include the selected linear regression models, the resulting estimates of the model coefficients, the associated statistics, and fitted propeller performance data obtained by application of the fits. Table 2 provides a description of the contents of the files.

Table 2: Description of the contents of the fitted data files.

Parameter	***Description***
a0 … aN	model coefficients
Estimate	coefficient estimate for each corresponding term in the model
SE	standard error of each of the coefficients
tStat	*t*-statistic for each coefficient; tests the null hypothesis that the corresponding coefficient is zero against the alternative that it is different from zero, given the other coefficients in the model (tStat = Estimate / SE)
pValue	*p*-value for the *t*-statistic of the hypothesis test that the corresponding coefficient is zero or not; model coefficient is only retained if *p*-value is smaller than 0.05 (i.e. significant at 5% significance level)
coefCIlow	lower limit for 95% confidence interval per model coefficient
coefCIhigh	upper limit for 95% confidence interval per model coefficient
Number of observations	number of data points used to define fit
Error degrees of freedom	difference between number of observations and number of coefficients in the model
Root mean squared error	square root of the mean squared error; estimates the standard deviation of the error distribution
R-squared	coefficient of determination (proportion of total sum of squares explained by the model)
Adjusted R-squared	adjusted coefficient of determination (accounts for number of model coefficients)

F-statistics vs. constant model	test statistic for the *F*-test on the regression model. Tests whether the model fits significantly better than a model consisting only of a constant term.
p-value	*p*-value for the *F*-test on the model
J	propeller advance ratio used to evaluate response (defined in Table 1)
CT	propeller thrust coefficient (defined in Table 1)
CTlo	lower 95% confidence bound on propeller thrust coefficient
CThi	upper 95% confidence bound on propeller thrust coefficient
CP	propeller power coefficient (defined in Table 1)
CPlo	lower 95% confidence bound on propeller power coefficient
CPhi	upper 95% confidence bound on propeller power coefficient
ETA	propeller efficiency (defined in Table 1)
ETAlo	lower 95% confidence bound on propeller efficiency
ETAhi	upper 95% confidence bound on propeller efficiency

8 Folder structure

The data folder contains documentation, geometry files, raw data files, corrected data files, and fitted data files. The data files are grouped in folders based on the considered blade pitch setting.

The raw data are collected in .csv files, one for each freestream-velocity setpoint. Separate files are made for the different propeller pitch settings considered.

For each freestream-velocity setpoint, response-surface models are generated for thrust coefficient and power coefficient as a function of advance ratio. For the data set at a freestream velocity of 0 m/s, the tip Mach number is used as independent variable instead of the advance ratio. The resulting models are presented in the fittedData files, together with examples of fitted data.

The folder structure is as follows:

- ./
  - README.pdf
- ./GEOMETRY
  - TUD_OJF_TUD-XPROP_beta0_7Rp20deg_propeller_assembly.stp
  - TUD_OJF_TUD-XPROP_beta0_7Rp30deg_propeller_assembly.stp
  - TUD_OJF_TUD-XPROP_beta0_7Rp45deg_propeller_assembly.stp
- ./DATA
  - ./BetaP070R20deg
    - TUD_OJF_TUD-XPROP_beta070R20deg_Vset00ms_rawData_Jsweeps.csv
    - TUD_OJF_TUD-XPROP_beta070R20deg_Vset06ms_rawData_Jsweeps.csv
    - TUD_OJF_TUD-XPROP_beta070R20deg_Vset12ms_rawData_Jsweeps.csv
    - TUD_OJF_TUD-XPROP_beta070R20deg_Vset18ms_rawData_Jsweeps.csv
    - TUD_OJF_TUD-XPROP_beta070R20deg_Vset00ms_fittedData_Jsweeps.csv
    - TUD_OJF_TUD-XPROP_beta070R20deg_Vset06ms_fittedData_Jsweeps.csv
    - TUD_OJF_TUD-XPROP_beta070R20deg_Vset12ms_fittedData_Jsweeps.csv
    - TUD_OJF_TUD-XPROP_beta070R20deg_Vset18ms_fittedData_Jsweeps.csv
  - ./BetaP070R30deg
    - TUD_OJF_TUD-XPROP_beta070R30deg_Vset00ms_rawData_Jsweeps.csv

        - TUD_OJF_TUD-XPROP_beta070R30deg_Vset06ms_rawData_Jsweeps.csv
        - TUD_OJF_TUD-XPROP_beta070R30deg_Vset10ms_rawData_Jsweeps.csv
        - TUD_OJF_TUD-XPROP_beta070R30deg_Vset12ms_rawData_Jsweeps.csv
        - TUD_OJF_TUD-XPROP_beta070R30deg_Vset15ms_rawData_Jsweeps.csv
        - TUD_OJF_TUD-XPROP_beta070R30deg_Vset18ms_rawData_Jsweeps.csv
        - TUD_OJF_TUD-XPROP_beta070R30deg_Vset20ms_rawData_Jsweeps.csv
        - TUD_OJF_TUD-XPROP_beta070R30deg_Vset25ms_rawData_Jsweeps.csv
        - TUD_OJF_TUD-XPROP_beta070R30deg_Vset30ms_rawData_Jsweeps.csv
        - TUD_OJF_TUD-XPROP_beta070R30deg_Vset00ms_FittedData.txt
        - TUD_OJF_TUD-XPROP_beta070R30deg_Vset06ms_FittedData.txt
        - TUD_OJF_TUD-XPROP_beta070R30deg_Vset10ms_FittedData.txt
        - TUD_OJF_TUD-XPROP_beta070R30deg_Vset12ms_FittedData.txt
        - TUD_OJF_TUD-XPROP_beta070R30deg_Vset15ms_FittedData.txt
        - TUD_OJF_TUD-XPROP_beta070R30deg_Vset18ms_FittedData.txt
        - TUD_OJF_TUD-XPROP_beta070R30deg_Vset20ms_FittedData.txt
        - TUD_OJF_TUD-XPROP_beta070R30deg_Vset25ms_FittedData.txt
        - TUD_OJF_TUD-XPROP_beta070R30deg_Vset30ms_FittedData.txt
    - ./betaP070R45deg
        - TUD_OJF_TUD-XPROP_beta070R45deg_Vset29ms_rawData_Jsweeps.csv
        - TUD_OJF_TUD-XPROP_beta070R45deg_Vset29ms_Jset1.4_rawData_AoAsweeps.csv
        - TUD_OJF_TUD-XPROP_beta070R45deg_Vset29ms_Jset1.6_rawData_AoAsweeps.csv
        - TUD_OJF_TUD-XPROP_beta070R45deg_Vset29ms_Jset1.8_rawData_AoAsweeps.csv
        - TUD_OJF_TUD-XPROP_beta070R45deg_Vset29ms_Jset2.0_rawData_AoAsweeps.csv
        - TUD_OJF_TUD-XPROP_beta070R45deg_Vset29ms_Jset2.2_rawData_AoAsweeps.csv
        - TUD_OJF_TUD-XPROP_beta070R45deg_Vset29ms_Jset2.4_rawData_AoAsweeps.csv
        - TUD_OJF_TUD-XPROP_beta070R45deg_Vset29ms_FittedData.csv

9 References

[1] Nahuis, R and Sinnige, T, “Design, manufacture and commissioning of a new NLR 6-component rotating shaft balance for Delft University of Technology,” *10th International Symposium on Strain-Gauge Balances*, Mianyang, China, May 2016.